

Received: 13 October 2016 Accepted: 28 December 2016 Published: 03 February 2017

# **OPEN** Longitudinal *in vivo* bioimaging of hepatocyte transcription factor activity following cholestatic liver injury in mice

Juliette M. K. M. Delhove<sup>1,3</sup>, Suzanne M. K. Buckley<sup>2</sup>, Dany P. Perocheau<sup>2</sup>, Rajvinder Karda<sup>2</sup>, Patrick Arbuthnot<sup>3</sup>, Neil C. Henderson<sup>4</sup>, Simon N. Waddington<sup>2,3</sup> & Tristan R. McKay<sup>1,5</sup>

Molecular mechanisms regulating liver repair following cholestatic injury remain largely unknown. We have combined a mouse model of acute cholestatic liver injury, partial bile duct ligation (pBDL), with a novel longitudinal bioimaging methodology to quantify transcription factor activity during hepatic injury and repair. We administered lentiviral transcription factor activated luciferase/eGFP reporter (TFAR) cassettes to neonatal mice enabling longitudinal TFAR profiling by continued bioimaging throughout the lives of the animals and following pBDL in adulthood. Neonatal intravascular injection of VSV-G pseudotyped lentivirus resulted in almost exclusive transduction of hepatocytes allowing analysis of hepatocyte-specific transcription factor activity. We recorded acute but transient responses with NF-κB and Smad2/3 TFAR whilst our Notch reporter was repressed over the 40 days of evaluation post-pBDL. The bipotent hepatic progenitor cell line, HepaRG, can be directed to differentiate into hepatocytes and biliary epithelia. We found that forced expression of the Notch inhibitor NUMB in HepaRG resulted in enhanced hepatocyte differentiation and proliferation whereas over-expressing the Notch agonist JAG1 resulted in biliary epithelial differentiation. In conclusion, our data demonstrates that hepatocytes rapidly upregulate NF-kB and Smad2/3 activity, whilst repressing Notch signalling. This transcriptional response to cholestatic liver injury likely promotes partial de-differentiation to allow pro-regenerative proliferation of hepatocytes.

The liver has a unique ability to regenerate. Hepatocytes represent approximately 85% of the liver mass, and are the major metabolic functional units of the liver. Therefore understanding more about the transcriptional regulation of hepatocyte biology, both in health and disease, is key to the rational design of new pro-regenerative therapies. Partial bile duct ligation (pBDL) in mice is a model of acute cholestatic liver injury, which results in increased biliary pressure followed by hepatic injury, inflammation and hepatocyte proliferation<sup>1</sup>. Cholestasis in mice results in the development of a ductular reaction involving neutrophil recruitment, focal zonal necrosis, hepatic progenitor cell (HPC) proliferation and differentiation and hepatic stellate cell (HSC) activation to a matrix-secreting myofibroblast phenotype (Reviewed in ref. 2). The role of resident macrophage Kupffer cells in contentious with depletion experiments in BDL models providing inconclusive data to their role<sup>3-5</sup>. HSC activation is known to be via a TGF-β1 and potentially Notch-dependent mechanism<sup>6</sup> whilst NF-κB signaling is known to induce hepatocyte proliferation after liver injury<sup>7</sup>. Interestingly, Kim et al. have recently shown that NF-κB can itself activate Notch signaling and proliferation in cholangiocytes8. CCN1/integrin-activated NF-κB leads to Jagged1/Notch signaling and proliferation of cholangiocytes after BDL. This mechanism also appears to activate HSCs to promote HPC proliferation and differentiation to cholangiocytes. Application of soluble JAG1 after BDL has been shown to reduce hepatic necrosis and ductular reaction<sup>8</sup>. Furthermore, following hepatic injury

<sup>1</sup>Stem Cell Group, Cardiovascular & Cell Sciences Research Institute, St. George's University of London, Cranmer Terrace, London SW17 0RE, UK. <sup>2</sup>Gene Transfer Technology Group, Institute for Women's Health, University College London, 86-96 Chenies Mews, London WC1E 6HX, UK. 3Wits/SAMRC Antiviral Gene Therapy Research Unit, Faculty of Health Sciences, University of the Witwatersrand, Johannesburg, South Africa. 4MRC Centre for Inflammation Research, The Queens Medical Research Institute, University of Edinburgh, Edinburgh EH16 4TJ, U.K. <sup>5</sup>School of Healthcare Sciences, Manchester Metropolitan University, Chester Street, Manchester M1 5GD, U.K. Correspondence and requests for materials should be addressed to S.N.W. (email: s.waddington@ucl.ac.uk)



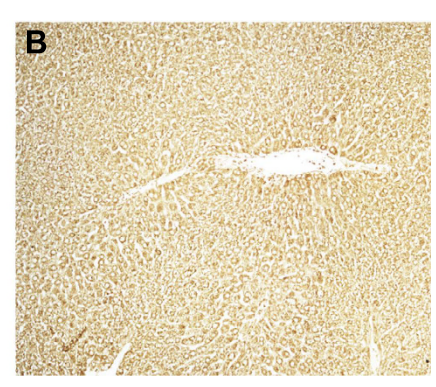


Figure 1. Neonatal intravascular administration of lentiviral vectors targets the liver and overwhelmingly transduces hepatocytes. Lentivirus constitutively expressing FLuc and GFP (LNT-SFFV-FLuc/eGFP) was administered to P1 neonatal mice by intravascular injection. Mice were sacrificed after 90 days and liver sections immunostained with GFP antibody. (A) GFP expression was overwhelmingly evident in hepatocytes compared to (B) controls (n = 3 both groups).

Wnt3a secretion from macrophages maintains the expression of the Notch inhibitor, Numb, in HPCs promoting their differentiation to hepatocytes<sup>9</sup>. A complex inter-relationship is emerging, which involves intracellular and paracrine signaling, controlling cell mobilization, proliferation and fate decisions in a context-dependent manner during liver development, homeostasis and injury.

We have developed an *in vivo* platform for quantifying hepatocyte transcription factor activity in live mice. We used lentiviral transcription factor activated reporter cassettes (TFAR) co-expressing firefly luciferase and eGFP. Conditional control of reporter gene activity by a synthetic promoter enabled longitudinal analysis of transcription factor activity profiles by continued bioimaging in mice following pBDL. Intravascular injection of VSV-G pseudotyped lentiviruses into newborn mice resulted in almost exclusive transduction of hepatocytes, which allowed analysis of hepatocyte-specific transcription factor activity. This has enabled us to longitudinally assess hepatocyte NF-κB, Smad 2/3, Notch and Wnt signaling activity *in vivo* following pBDL. We then combined TFAR bioimaging with complementary immunohistochemistry and *in vitro* evaluation of hepatic progenitor cell (HepaRG cells) differentiation to provide new insights into the temporal transcriptional activity and signaling mechanisms that mediate the hepatic injury and repair response during cholestatic liver injury.

#### Results

**Lentiviral transduction is restricted largely to hepatocytes after intravenous administration to neonatal mice.** Here we report, for the first time, that intravenous administration of VSV-G pseudotyped lentivirus constitutively expressing FLuc/eGFP in P0 mouse neonates results in efficient liver-restricted hepatocyte transduction (Fig. 1A and B) that is maintained for over 100 days<sup>10</sup>. Bile duct ligation is an established model for initiation of the ductular reaction. However, complete occlusion of the common bile duct in mice can result in severe hepatic injury, liver failure and mortality. Partial bile duct ligation (pBDL) can be achieved by either a partial occlusion of the common bile duct<sup>11</sup> or a complete occlusion of the ducts draining the median and left liver lobes leaving the right and caudate lobes fully functional<sup>12</sup> and therefore we used pBDL throughout this study. Following pBDL, we observed bile duct dilatation, biliary hyperplasia, and mononuclear cell infiltrate characteristic of portal tract ductular reaction (Fig. 2Ai and ii). Furthermore, an increase in collagen deposition was observed following pBDL (Fig. 2Bi and ii).

We initially administered a VSV-G pseudotyped lentivirus constitutively expressing FLuc/eGFP from the SFFV promoter to neonatal mice, which upon maturity, were subjected to pBDL or sham surgery followed by continued luciferase bioimaging. There was no difference in luciferase activity between pBDL and sham-treated animals. Similarly there was no change in reporter activity for up to 40 days post pBDL (Fig. 3A). Mice were sacrificed 90 days later to correlate lentiviral transduction with liver pathology at the cellular level. Intravenous administration of lentivirus resulted in up to 49% GFP positive hepatocytes. The vast majority of cells stably expressing eGFP 90 days post-pBDL were HNF4 $\alpha$ <sup>+</sup> hepatocytes (Fig. 3Bi-iii) Areas of ductular reaction were distinctly lacking in GFP expression. Furthermore GFP expression did not co-localise with markers of cholangiocytes (CK7, Fig. 3Ci-iii), hepatic progenitor cells (HPC – PKM2, Fig. 3Di-iii), myofibroblasts ( $\alpha$ -SMA, Fig. 3Ei-iii) or quiescent hepatic stellate cells (HSC – GFAP, Fig. 3Fi-iii).

**Hepatocyte specific TFAR activity after pBDL in adult mice.** In this study we used our previously described liver-targeted transcription factor activated reporter (TFAR) cassettes <sup>10</sup> to investigate hepatocyte-specific signalling during acute cholestatic liver injury. We have previously generated a library of lentiviral TFAR where serial transcription factor consensus sites are engineered upstream of a minimal promoter sequence driving a bicistronic firefly luciferase (FLuc)/eGFP reporter cassette (Fig. 4A). For this study we employed TFARs that were specific for four cell signalling pathways implicated in responses to cholestatic liver injury: NF- $\kappa$ B, TGF- $\beta$  (Smad2/3), Wnt (TCF/LEF) and Notch. We initially validated each TFAR for activation over 72h in HEK293T cells. NF- $\kappa$ B, TGF- $\beta$  and Wnt were all responsive to their respective agonists (LPS, Activin

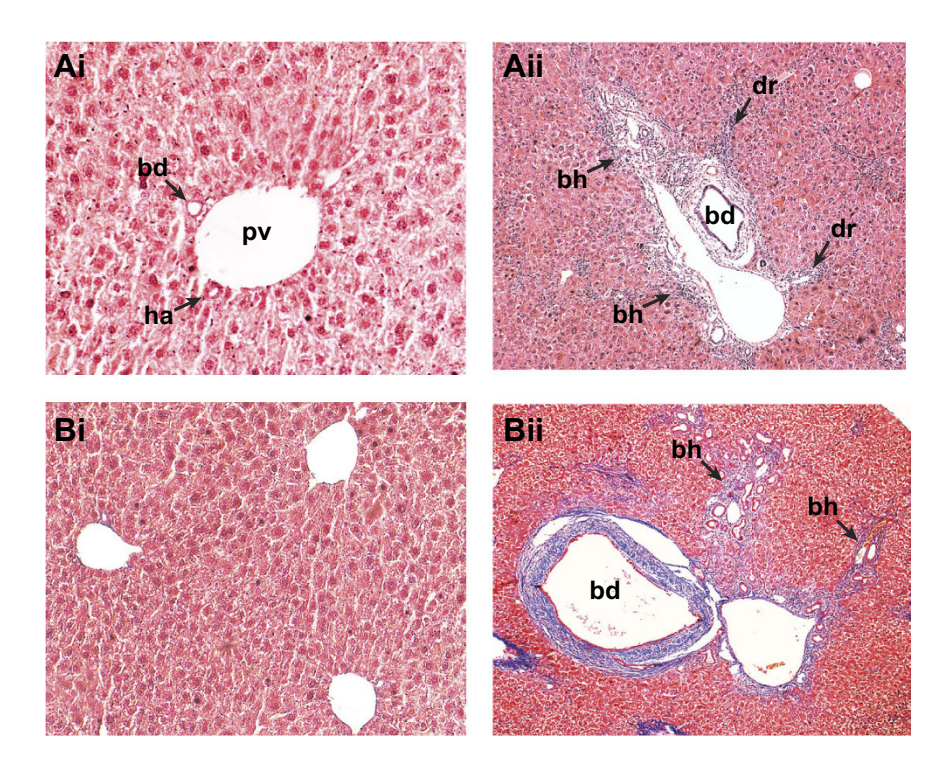


Figure 2. Partial bile duct ligation results in liver remodelling and collagen deposition in occluded lobes. Adult mice were subjected to partial bile duct ligation and sacrificed after 90 days. Control livers from sham operated mice (Ai) and occluded pBDL livers (Aii) were fixed, sectioned and stained with Hematoxylin & Eosin for histological architecture and Lilly's trichrome (Bi & ii) staining collagen (blue), nuclei (black) and cytoplasm (red). Bile duct (bd), portal vein (pv), biliary hyperplasia (bh), ductular reaction (dr), (n = 3 both groups).

A and LiCl2 respectively) (Fig. 4B–D) and Notch TFAR transduced cells were responsive to co-culture with JAG1 over-expressing 293 T cells in a dose dependent manner (Fig. 4E).

In vivo transcription factor activity analysis was performed by neonatal administration of lentivirus containing the biosensing TFAR. Signalling pathway activation during disease induction was then quantified as photonic output (schematically represented in Fig. 5A). Having shown that lentiviral transduction is almost exclusively hepatocyte-specific and maintained in daughter cells because of stable genomic integration of the expression cassette, we can assume that the expansion of FLuc/eGFP expression we observe during development is largely from hepatocytes. Our data generated using a constitutively activated GFP also suggest that following pBDL, most of the resident hepatocyte population survives and remains stable during liver remodelling post pBDL.

We next carried out longitudinal luciferase bioimaging in mice containing each of the four TFAR (NF- $\kappa$ B, TGF- $\beta$  (Smad2/3), Wnt (TCF/LEF) and Notch) following pBDL at 49–60 days post-birth. We observed an acute NF- $\kappa$ B response immediately after pBDL which was not apparent in sham operated controls (Fig. 5Bi and ii). Control mice were subjected to laparotomy to correct for any paracrine inflammatory response consequent to the abdominal surgery. Interestingly, in a number of the sham treated mice an NF- $\kappa$ B response in hepatocytes above baseline was observed that quickly diminished (Supplementary Fig. 1). This would be consistent with a systemic inflammatory response to the laparotomy. The NF- $\kappa$ B response peaked 10 days after pBDL and decreased to baseline by 24 days. This was revealed by a more than 28-fold increase in NF- $\kappa$ B activity following pBDL when compared to controls, as revealed by analysis of the area under curve. A similar statistically significant, but less pronounced, response was seen with the TGF- $\beta$  activated Smad2/3 TFAR at the same timepoints (Fig. 5Ci and ii). Collectively, these data demonstrate that hepatocytes are important "primary responders" to inflammatory and fibrotic stimuli following biliary injury.

The Notch and Wnt pathways have been implicated in regeneration and repair after hepatic injury. To analyse the role of these pathways following pBDL, adult liver targeted TFAR mice were assessed by continued bioimaging as before. The Notch TFAR mice showed a prolonged and significant decrease in luciferase reporter activity in pBDL compared to sham-treated animals (Fig. 6Ai and ii) but the Wnt activated TCF/LEF TFAR showed no significant change in activity (Fig. 6Bi and ii). Histological assessment of activated NICD and  $\beta$ -catenin showed largely membrane-bound localization in cholangiocytes in sham and pBDL-treated mice (Fig. 6C and D). Collectively, these data indicate that hepatocyte Notch transcription factor activity is decreased following pBDL, and notch signalling is localized to the bile ducts in normal and hyperplastic livers after pBDL. It is possible that hepatocytes inhibit Notch signals that are emanating from hyperplastic bile ducts in pBDL livers.

**Interrogation of Wnt and Notch signalling in differentiated HepaRG cultures.** To interrogate the interactions of hepatocytes and cholangiocytes we exploited the bipotent nature of the HepaRG cell line. Bipotent HepaRG progenitors were subjected to a differentiation protocol previously described by Dianat *et al.*<sup>13</sup>.

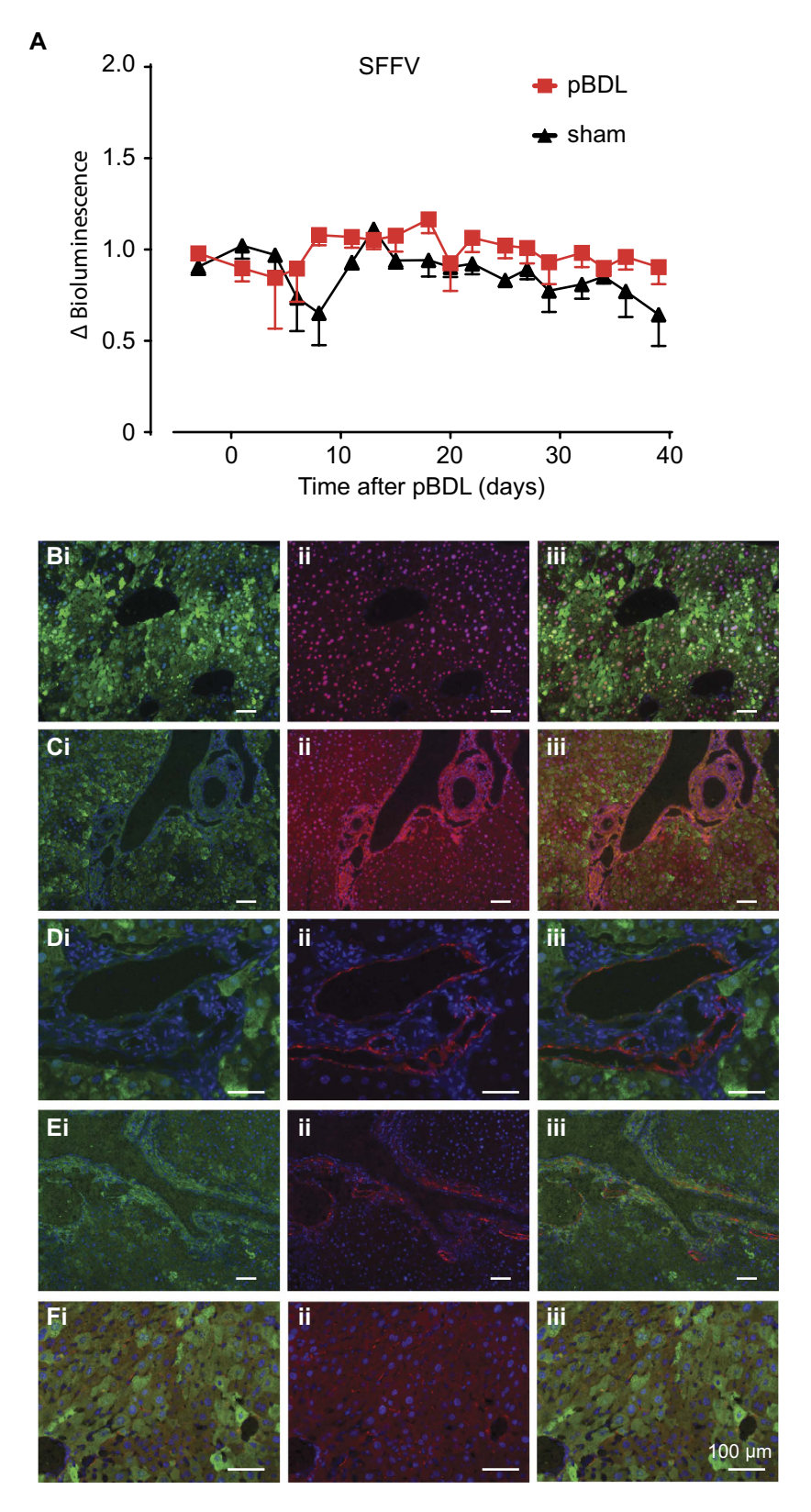


Figure 3. Reporter gene expression is stable and restricted to hepatocytes after pBDL following neonatal intravascular administration of lentiviral vectors. SFFV-FLuc/eGFP lentivirus was administered to P1 neonatal mice by intravascular (i.v.) injection and then subjected to pBDL or sham pBDL in adulthood. (A) Mice were subjected to continued luciferase bioimaging over 40 days where no change in luciferase activity was observed over time or between pBDL and sham groups (n = 10 pBDL, 5 sham, not significant, Student's t-test). Mice were sacrificed 90 days after pBDL and co-immunostained for GFP and markers of (Bi-iii) hepatocytes; HNF4 $\alpha$ , (C-iii) biliary epithelia; CK7, (Di-iii) hepatic progenitors; PKM2, (Ei-iii) myofibroblasts;  $\alpha$ SMA and (Fi-iii) hepatic stellate cells; GFAP (all groups n = 3–6).

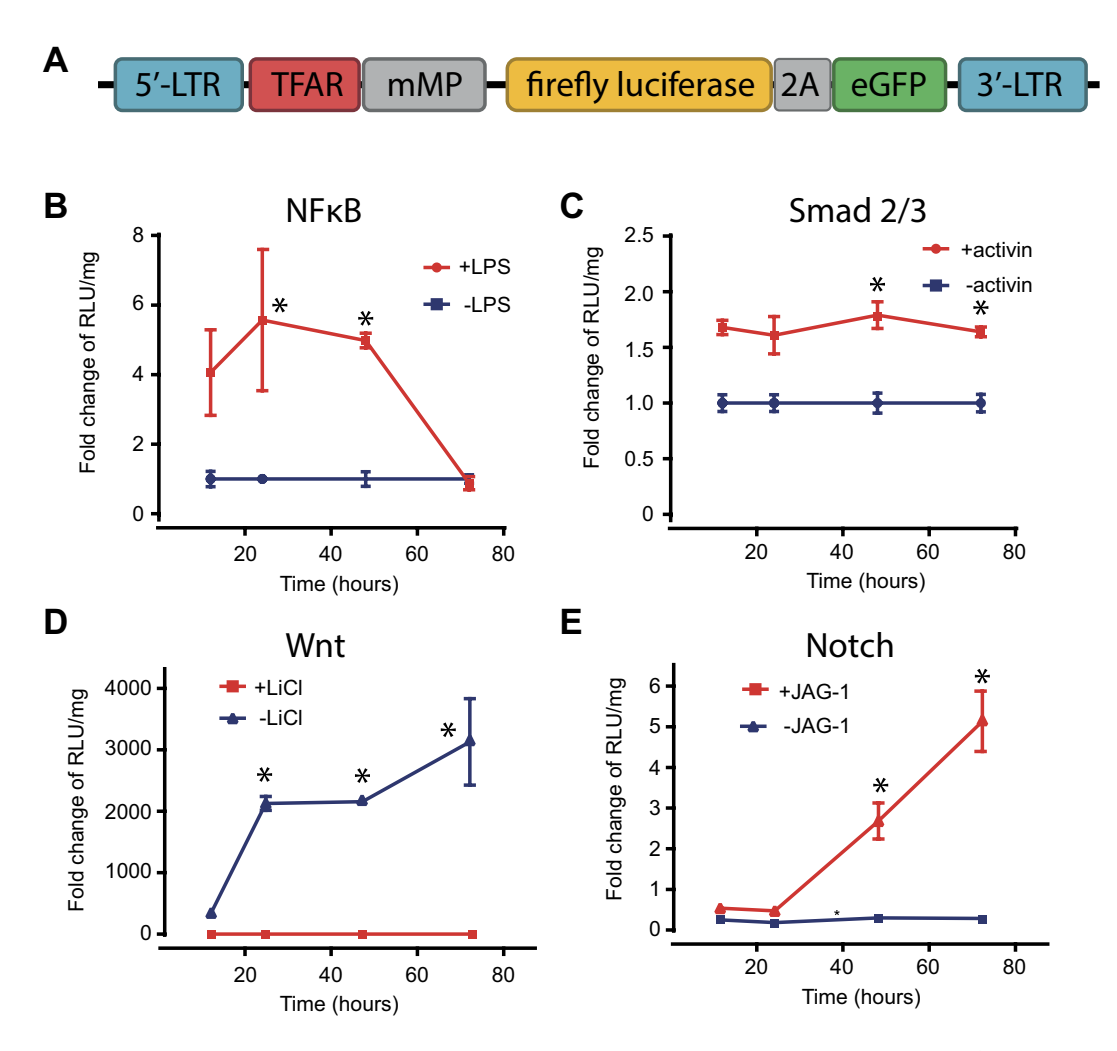


Figure 4. *In vitro* validation of transcription factor activated lentiviral reporter vectors. (A) Schematic representation of parental lentiviral reporter construct. (B–E) 293 T cells were transduced with VSV-G pseudotyped TFAR lentiviral vectors at an MOI of 10 then incubated with the relevant agonists and luciferase expression quantified at 12, 24, 48 and 72 h (n = 3-6, mean+/- SEM, comparison by analysis of variance with repeated measures).

The protocol was developed to differentiate HepaRG to cholangiocytes but in our hands it reproducibly generated CK19+ cholangiocyte cultures interspersed with colonies of HNF4 $\alpha$ +/ALB+ hepatocytes (Fig. 7Ai–iv). In agreement with our evaluations *in vivo*, we observed widespread membrane-bound  $\beta$ -catenin staining in CK19-positive cholangiocytes and interestingly, increased NICD staining at the interface between cholangiocytes and the hepatocyte colonies (Fig. 7Av and vi). We compared the effects of modulating Notch signalling by transducing HepaRG cells with lentiviruses constitutively expressing the Notch inhibitor NUMB (HepaNumb) or the Notch ligand JAG1 (HepaJag) before subjecting them to our differentiation protocol. There was a significantly higher total area of hepatocyte-like colonies in HepNumb cultures (36.94%, n = 14) compared to HepaJag (22.05%, n = 12) (Fig. 7Bi and ii). The transgenes were expressed from a bicistronic lentiviral cassette co-expressing GFP from a truncated CMV promoter and transduction efficiencies ranged between 50 and 80%. Interestingly, we did not observe Jag1/GFP expression in any hepatocyte-like colonies (Fig. 7Ci and ii). We imply from these data that hepatocyte differentiation can only occur in HepaRG cells when Notch activity is repressed. This is consistent with increased hepatocyte colony formation in Numb transduced HepaRG cultures.

#### Discussion

Bile duct ligation in rodents results in acute cholestasis and a ductular reaction with upregulation of inflammatory and pro-fibrotic signalling  $^{14}$ . Complete ligation of the common bile duct causes high rates of mortality but partial bile duct ligation (pBDL), occluding the ducts draining the left and median lobes, results in localized cholestasis that is amenable to longer-term analysis  $^{15}$ . NF- $\kappa$ B and TGF- $\beta$ 1 signaling are prominent in promoting responses to liver injury such as myofibroblastic differentiation and ECM remodelling  $^{16,17}$ . Although the role of TGF- $\beta$  signaling is well characterised in HSC, activity in hepatocytes after liver injury is less clear. Two previous studies have indicated that following liver injury TGF- $\beta$  signalling emanates from hepatocytes but neither present a longitudinal analysis  $^{17,18}$ . We sought to investigate longitudinal transcription factor activity *in vivo* using bioluminescence imaging in live mice subjected to pBDL. A constitutively activated eGFP reporter was used to assess

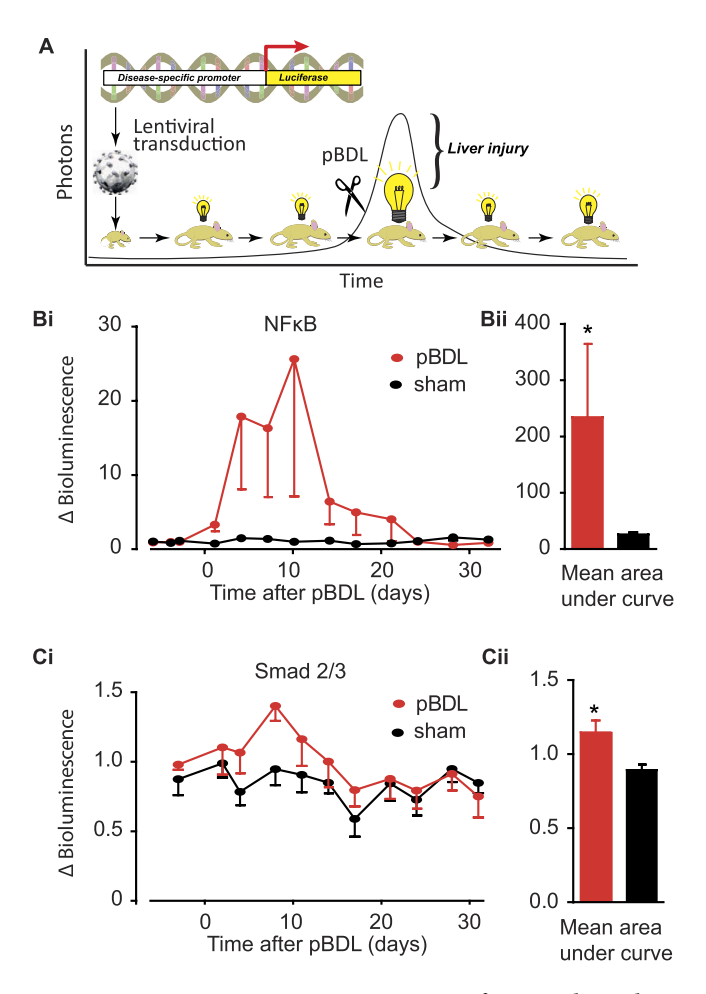


Figure 5. pBDL causes transient activation of NFB and Smad2/3 transcription factor activity. (A) Cartoon of the principles underlying somatotransgenic bioimaging. Lentiviruses expressing transcription factor activated reporter (TFAR) constructs expressing luciferase and GFP are administered to neonates. When they reach adulthood baseline luciferase expression is assessed before inducing a disease state, in this case by pBDL. Continued luciferase bioimaging provides a quantifiable surrogate for nuclear localization and target DNA binding of transcription factors. Somatotransgenic mice were generated as described then subjected to pBDL or sham pBDL and luciferase activity assayed over 30 days. (Bi & ii) NFkB and (Ci & ii) Smad2/3 TFAR activity showed significant increases as assessed by area under the curve analysis (NFkB, n = 13 pBDL, n = 6 sham; p < 0.0001; Smad2/3, n = 9 pBDL, n = 9 sham, p < 0.05, Student's t-test).

the distribution of lentiviral transduction > 90 days post-transduction. In line with our previous observations, transduction was largely restricted to the liver but, unexpectedly, histological analysis revealed that transduced cells within the liver were almost exclusively hepatocytes. Specifically, we observed no evidence of cholangiocyte, HSC or HPC transduction pre- or post-BDL inferring that we were not transducing bi-potent progenitor cells. This provided us with a unique tool to assess transcription factor activity specifically in hepatocytes subsequent to pBDL.

Bile duct ligation results in an acute phase inflammatory response leading to necrosis <sup>19</sup> caused directly by bile acid reflux<sup>20</sup> and other deregulated factors such as osteopontin<sup>21</sup>. There is strong evidence from mice that NF-κB activation during this inflammatory phase promotes hepatocyte proliferation *in vivo* following partial hepatectomy<sup>7,22</sup>. In hepatocytes we saw an acute increase in both NF-κB and Smad2/3-mediated luciferase activity after pBDL, peaking at around 10 days post-BDL before returning to pre-pBDL levels at 28 days. Interestingly, NF-κB and Smad2/3 responses returned to pre-pBDL levels within the same timeframe, whereas it is known that liver fibrosis in partial BDL models progresses over many months<sup>23</sup>. This would suggest that compensatory factors restore a homeostatic balance to reduce damage and maintain function despite chronic disease. This would be consistent, for example, with Smad7 upregulation repressing Smad2/3 responses despite continued expression of TGF- $\beta$ 1<sup>17</sup>. Although the role of TGF- $\beta$  signalling in hepatocytes is not clearly understood it is well established that TGF- $\beta$  promotes the ductular reaction in BDL rats by promoting cholangiocyte proliferation in an  $\alpha$ v $\beta$ 6-integrin specific manner<sup>24,25</sup>. Our data is the first hepatocyte-targeted description of NF-κB and Smad2/3 activated luciferase reporter bioimaging in a rodent pre-clinical model of acute cholestatic liver injury.

Notch signalling is established as playing a significant role in bile duct development where the Notch ligand JAG1 promotes cholangiocyte differentiation of bi-potent HPCs<sup>26</sup>. NF-κB and Notch signalling have been linked

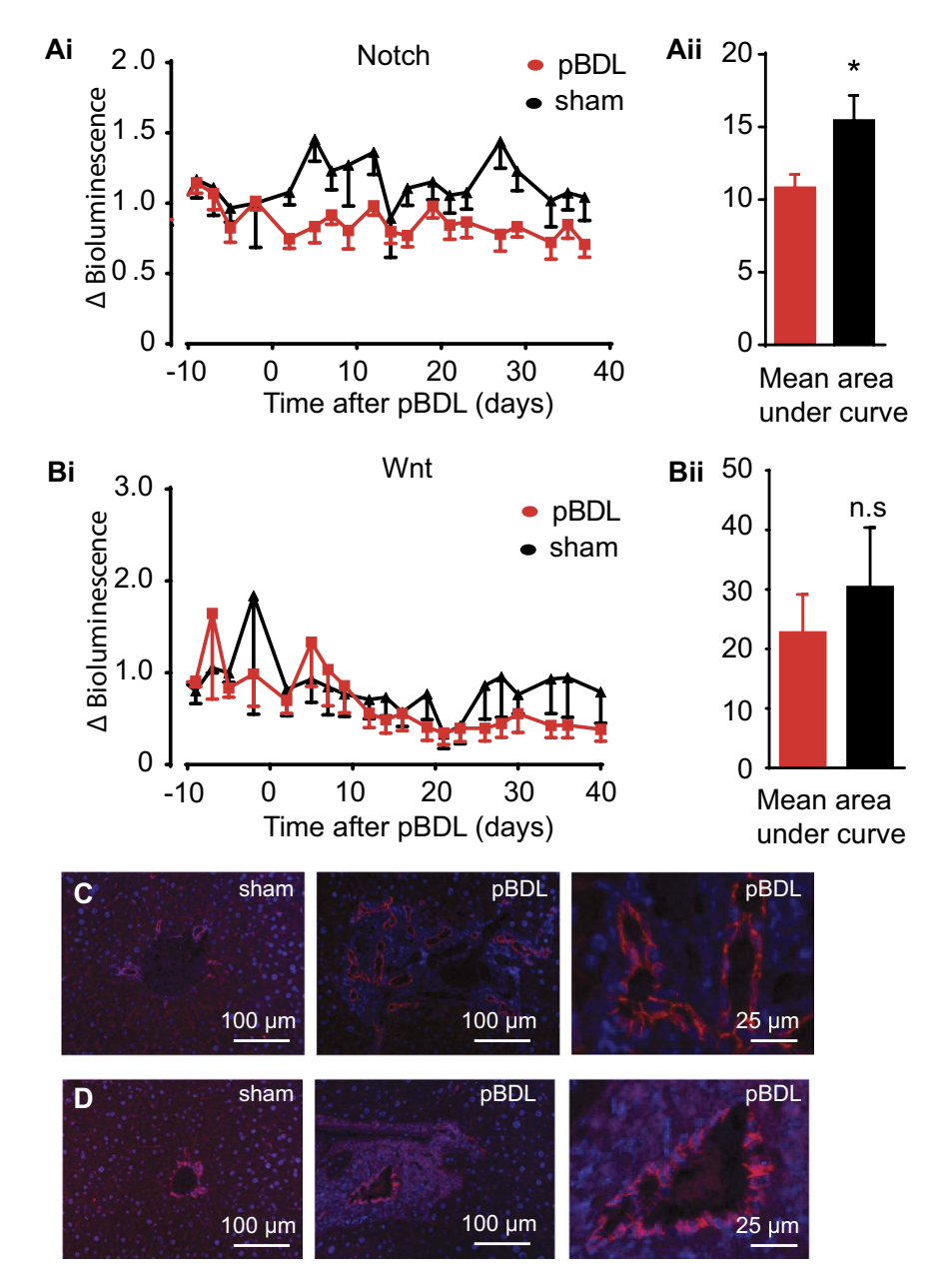


Figure 6. pBDL causes repression of Notch signalling. Mice somatotransgenic for liver specific expression of the Notch and Wnt (TCF/LEF) TFAR were subjected to pBDL or sham surgery. There was significant repression of the (Ai & ii) Notch TFAR over 40 days pBDL compared to sham control analysed by area under the curve comparison (n = 10 pBDL, n = 5 sham; p < 0.05, Student's t-test) but no significant change in (Bi & ii) Wnt TFAR activity (n = 8 pBDL, n = 5 sham, not significant, Student's t-test). Immunohistochemistry of liver sections 90 days after pBDL showed an increase in the number of (C) NICD positive and (D)  $\beta$ -Catenin positive bile ducts in pBDL compared to sham (n = 3).

during HPC commitment to cholangiocytes during the ductular reaction in mice<sup>8</sup>, and also to the severity of human hepatic fibrosis<sup>6</sup> but never related specifically in hepatocytes after pBDL. Haploinsufficiency at the locus encoding the Notch ligand JAGI results in Alagille syndrome characterised by impaired intrahepatic bile duct development and widespread ductular reaction. There is no obvious effect on hepatocytes<sup>27</sup> and Notch inhibition by Wnt3a-mediated Numb upregulation in HPCs results in hepatocyte specification<sup>9</sup>. Our longitudinal assessment indicated that Notch signalling is actually inhibited in hepatocytes over 50 days post-pBDL whilst there is no change in Wnt-mediated TCF/LEF activity throughout a similar timecourse. Immunohistochemistry showed that both  $\beta$ -catenin and NICD present in cholangiocytes but largely absent from hepatocytes. The absence of NICD in hepatocytes is consistent with upstream inhibition of Notch receptor cleavage as protection from perpetuating Notch signalling emanating from the ductular reaction.

 $Transduction \ of the \ bi-potent \ hepatic \ progenitor \ cell \ line \ HepaRG \ with \ lentiviruses \ constitutively \ expressing \ Numb \ or \ JAG1 \ further \ corroborates \ this \ hypothesis. \ Numb \ over-expression \ resulted \ in \ an \ increase \ in \ the$ 

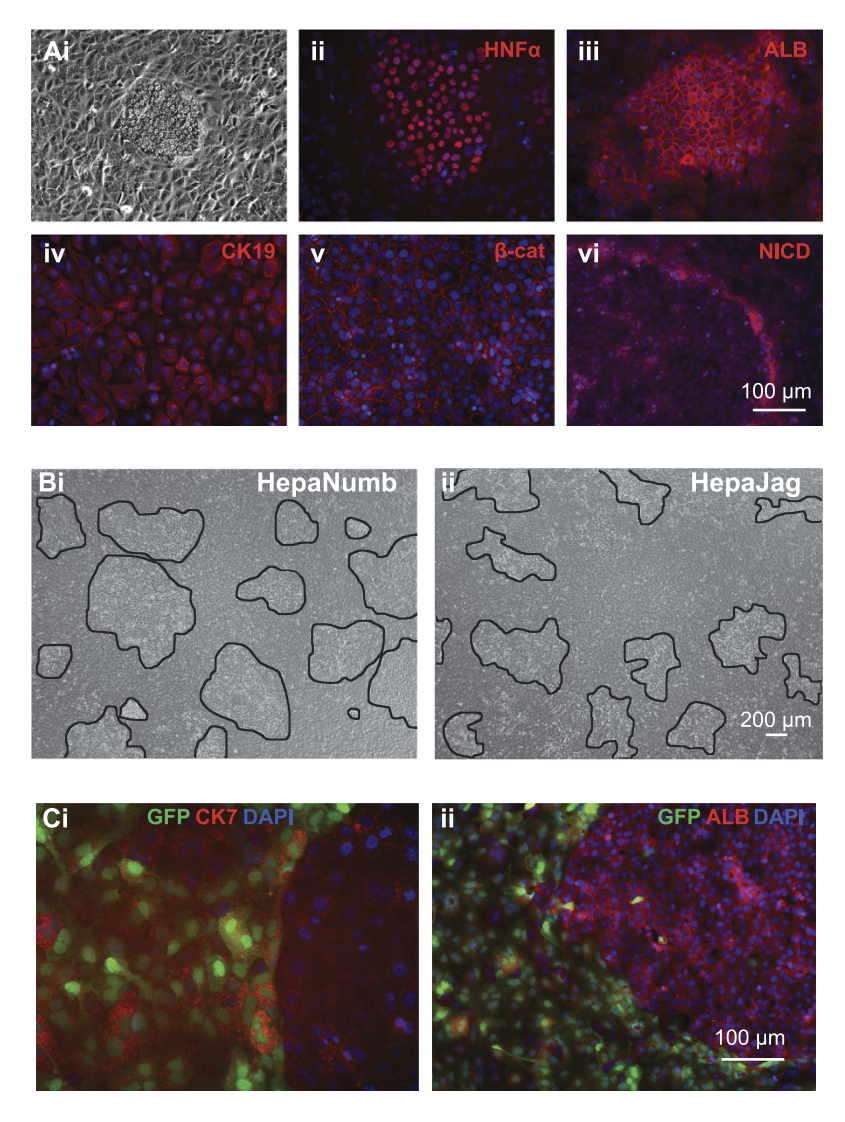


Figure 7. Modulation of Notch signalling influences the differentiation of bipotent HepaRG cells. HepaRG cells subjected to differentiation conditions formed (Ai) tight colonies that immunostained positive for the hepatocyte markers (Aii) HNF4 $\alpha$  and (Aiii) Albumin whereas the surrounding cells immunostained positive for the biliary epithelial marker (Aiv) CK19 and (Av)  $\beta$ -Catenin. The interface between colonies and surrounding cells immunostained positively for (Avi) NICD. Bipotent HepaRG cells were transduced with lentiviral constructs expressing Numb or Jag1/GFP then subjected to differentiation conditions. We observed a greater area of hepatocyte-like colonies in (Bi) HepaRG-Numb cells compared to (Bii) HepaRG-Jag1/GFP cells as quantified by total area ImageJ software. In HepaRG-Jag1/GFP cultures dual immunocytochemistry revealed that (Ci) GFP and CK7 co-localized but (Cii) GFP and Albumin never co-localized.

frequency and size of  $ALB^+/HNF4\alpha^+$  clusters seen within differentiated cultures compared to controls, indicating that reduced Notch signalling confers a propensity for cells to differentiate towards the hepatocyte lineage. Differentiated HepaRG cultures over-expressing JAG1 had less hepatocyte-like colonies. Interestingly, bi-potent HepaRG transduced with the JAG1-GFP expressing lentivirus were unable to differentiate to hepatocyte colonies. It is possible that this observation is a result of differential methylation of the CMV promoter in hepatocytes compared to cholangiocytes, or that hepatocyte differentiation is not possible in the presence of JAG1. With either situation hepatocyte-like colonies do not have exogenous JAG1 expression. There is some evidence that Notch inhibition promotes hepatocyte proliferation and in some cases metastases<sup>28,29</sup> implying hepatocytes are intrinsically resistant to Notch signalling <sup>30</sup>. The emerging consensus is that regenerative hepatocyte proliferation after acute liver injury does not emanate from progenitors residing within the canal of Hering <sup>31</sup>. Overall, our novel data highlights the use of longitudinal luciferase bioimaging in monitoring cell-type specific transcriptional activity in live animals. This has enhanced our understanding of the temporal activity profiles of the core transcriptional networks involved during acute cholestatic liver injury and repair.

Antibody	Supplier	Dilution
Mouse αCK19	Dako (M0888)	1:200
Mouse αCK7	Sigma (4465 P)	1:200
Mouse αHNF-4α	Perseus (PP-H1415-00)	1:200
Mouse αALB	R&D Systems (MAB1455)	1:200
Goat αSox9	R&D Systems (AF3075)	1:500
Rabbit αNICD	Abcam (ab8925)	1:200
Rabbit (active) β-catenin	New England Biolabs (8814S)	1:200
Rabbit α-goat Alexafluor	Life Technologies (A11079)	1:500
Goat α-rabbit Alexafluor	Life Technologies (A11011)	1:500
Goat α-mouse Alexafluor	Life Technologies (A11031)	1:500
DAPI	Sigma Adlrich (D9542)	1:1000

Table 1. Primary and secondary antibody information used for immunocytochemistry.

### Methods

**Construction and production lentiviral reporter vectors.** The NF- $\kappa$ B, SMAD2/3, Notch and Wnt (TCF/LEF) TFAR lentiviral vector cassettes were previously described in Buckley *et al.*<sup>10</sup>.

HEK293T viral producer cells were seeded at  $2\times10^7$  cells per T175 cm² flask and transfected using  $50\,\mu g$  pLNT-TFBE-JDG, 17.5  $\mu g$  pMD2.G (VSV-G envelope plasmid), and 32.5  $\mu g$  pCMV $\Delta$ R8.74 (gag-pol packaging plasmid) pre-complexed with 1  $\mu$ l polyethylenimine (10 mM) (Sigma-Aldrich) in OptiMEM for 3 h. Transfection media was replaced with complete DMEM and viral supernatant collected at 48 and 72 hours, filter sterilized (0.45  $\mu$ M), and concentrated by overnight low-g centrifugation. Pellets were resuspended in OptiMEM and stored at  $-80\,^{\circ}$ C. All viruses were titered using a p24 assay (Zeptometrix, Buffalo, NY, USA) as per manufacturer's instructions.

In vitro validation of reporter gene activity. HEK293T, HeLa and NIH3T3 cells were cultured in DMEM supplemented with 10% FBS, 1% penicillin/streptomycin (Sigma), 2mM L-glutamine and 1x non-essential amino acids. HepaRG cells were cultured in William's E medium containing Glutamax and sodium pyruvate supplemented with 10% FBS, 1% Pen/Strep, 1x non-essential amino acids,  $4\,\mu\text{g/ml}$  human recombinant insulin zinc solution, and  $50\,\mu\text{M}$  hydrocortisone. All reagents were sourced from Life Technologies.

For the *in vitro* validation of NF-κB, SMAD2/3 and Wnt (TCF/LEF) TFAR, cells were transduced with VSV-G pseudotyped lentivirus reporters at an MOI of 10. Small molecule or growth factor agonists or inhibitors were used for reporter functional validation. The trophoblast-isolated SGHPL5 cell line was transduced with a Notch reporter lentivirus to validate this vector. Varying seeding densities of *JAGGED-1*-overexpressing HEK293T cells were used to activate the Notch-SGHPL5 cells. Analysis was performed following 72 hours of co-culture.

Gene activation was quantified by luciferase assay on cell lysates as follows:  $20\,\mu l$  assay buffer (25 mM Tris phosphate pH 7.8, 1 mM DTT, 1 mM EDTA, 1% Triton X-100, 8 mM MgCl<sub>2</sub>, 3 ml glycerol, 1.25 mM rATP, 0.5% BSA) was added to  $20\,\mu l$  cell extract. Luciferin (Gold Biotechnology, MO, USA) was added to a final concentration of 1.5 mM and luminescence measured using the POLARstar Omega microplate reader (BMG Labtech). Analysis performed using MARS data analysis software (BMG Labtech). Relative light units were normalized relative to total protein as determined by Bradford assay (BioRad) using manufacturer's instructions.

Differentiation of HepaRG cells. HepaRG cells were seeded at low density and maintained in William's E medium containing 10% FBS, 1x non-essential amino acids, hydrocortisone ( $50\,\mu\text{M}$ ) and insulin ( $4\,\mu\text{g/ml}$ ). Cells were plated onto collagen-coated plates and allowed to grow to confluency prior to chemical induction. Confluent cells were treated with IL-6 ( $10\,\text{ng/ml}$ ) (R&D Systems) for 2 days, followed by 2 days of sodium taurocholate hydrate ( $10\,\text{nM}$ ) (Sigma) treatment, and a further 8 days of sodium taurocholate hydrate ( $10\,\text{nM}$ ) (Sigma) and sodium butyrate ( $1.8\,\mu\text{M}$ ) (Sigma) treatment.

**Immunocytochemistry.** Media was removed and cells washed 3x in PBS. Cells were fixed in 4% paraformaldehyde (PFA) (Sigma) for 20 minutes followed by three washes in PBS. Cells were incubated in blocking buffer (PBS, 0.3% Triton X-100, 1% BSA) for one hour at room temperature before the addition of primary antibody (Table 1) resuspended in blocking buffer was added to the cells and incubated overnight at 4 °C. Cells were washed three times in PBS for 5 minutes followed by incubation at room temperature for 1 hour with fluorophore-conjugated secondary antibody resuspended in blocking buffer. Cells were washed 3x in PBS and incubated in  $1 \times 4'$ ,6-diamidino-2-phenylindole (DAPI)(Sigma) in PBS for 5 minutes before being washed 3x in PBS for 5 minutes. Cell F imaging software was used for all analysis.

**Animal procedures.** Unless otherwise stated, outbred CD1 mice (Charles River) were time mated to produce neonatal animals. At postnatal day 1, neonates were briefly anesthetized (on ice) and lentivirus injected by intravenous (via the superficial temporal vein) injection.

All experiments were performed in accordance with relevant guideless and regulations: Experiments were carried out under United Kingdom Home Office regulations and approved by the ethical review committees of Imperial College London and University College London.

Antibody	Supplier	Antigen Retrieval	Dilution
Chicken αGFP	NEB (13970)	Na Citrate (pH6)	1:300
Mouse αCK7	Perseus (PP-H415-00)	Na Citrate (pH6)	1:200
Mouse αHNF-4α	Dako (M0851)	Tris HCl (pH10)	1:100
Rabbit αSMA	Dako (Z0334)	Na Citrate (pH6)	1:200
Rabbit αGFAP	Dako (M7018)	Tris HCl (pH10)	1:500
Rabbit α-PKM2	Life Technologies (PA5-23034)	Na Citrate (pH6)	1:200
Goat α-rabbit Alexafluor	Life Technologies (A-11011)		1:500
Goat α-mouse Alexafluor	Life Technologies (A-11031)		1:500
Goat α-chicken Alexafluor	R&D Systems (NL018)		1:400
DAPI	Sigma Aldrich (D9542)		1:1000

Table 2. Primary and secondary antibodies used for immunohistochemistry.

Partial bile duct ligation in mice. At 49 (SFFV), 50 (NF- $\kappa$ B, Wnt, Notch), or 60 (Smad 2/3) days post-birth, mice were anaesthetized with isoflurane (Abbott Laboratories) and a midline laparotomy ( $\approx$ 15 mm) performed just caudal to the sternum. The median and left lobes of the liver were exteriorized and kept moist with sterile gauze. The bile duct was ligated with 6–0 silk suture to occlude outflow from the left and median lobes but not occluding bile outflow from the right and caudate lobes as described by Yang and colleagues<sup>32</sup>. The liver was returned to the abdomen and the wound closed in two stages using 6–0 silk suture; skin was closed using a subcuticular suture with buried knots. Sham operated mice received laparotomy only. Mice were allowed to recover in a warmed chamber. Pre- and post-operative buprenorphine analgesia was provided.

**Bioluminescence imaging.** Unless otherwise stated, mice were anaesthetized with isoflurane (Abbott Laboratories), injected i.p. with firefly D-luciferin (15 mg/ml in PBS; Gold Biotechnology) and imaged 5 min later with a cooled charge-coupled device (CCCD) camera (IVIS; PerkinElmer). Luciferin dose was 150 mg/kg; volume varied with age/size of animal, for example, adult mice were given 300μl. Grey-scale photographs were acquired with a 24-cm field of view and then a bioluminescence image was obtained using a binning (resolution) factor of 4, a 1.2/f stop and open filter. Regions of interest (ROIs) were defined manually using a standard area for each organ under investigation. Signal intensities were calculated with Living Image software (Perkin Elmer) and expressed as photons per second per cm² per steradian. Where possible, BLI was carried out in adult reporter rodents on three consecutive days to establish a robust median baseline; subsequent data points were expressed as fold-change over this internal standard for each individual animal.

**Immunohistochemistry.** Liver tissue was fixed in 10% formalin overnight, dehydrated using 70%, 80%, 90% and  $2 \times 100\%$  ethanol for 1 hour each followed by Histoclear (National Diagnostics) overnight. Samples were embedded in Fibrowax (VWR). Tissue sections were cleared twice in Histo-clear for 10 minutes each, and brought to water using 90%, 70%, and 50% IMS, followed by 5 minutes in distilled water. Antigen retrieval was performed in 10 mM citrate buffer (pH6.0)(Sigma-Aldrich) or 10 mM Tris HCL for 40 or 10 minutes respectively and cooled for 20 minutes. Samples were incubated for 10 minutes in TBS containing 0.3% Triton X-100 (TBS-T) followed by blocking in TBS-T + 15% normal goat serum (NGS) (Vector laboratories) for 1 hour at room temperature. Primary antibody (see Table 2) was diluted in TBS-T/10% NGS overnight at 4 °C. Slides were rinsed thrice for 5 minute in TBS followed by incubation in secondary antibody diluted in TBS-T/10% NGS for 1 hour at room temperature. Samples were washed thrice for 5 minutes in TBS before incubation with 0.3% Sudan Black B made up in 70% ethanol for 15 minutes at room temperature. Sections were rinsed thrice with TBS for 5 minutes and mounted using Fluorescence Mounting Medium (Dako). Images in several fields were quantified using ImageJ software as outlined by Wang *et al.*<sup>33</sup>. Images were subjected to thresholding to determine true GFP expression over background with pixels between background level (79) and the maximum (255) considered positive. Positive pixels as a percentage of total image pixels were used to determine total area of GFP positive regions.

**H&E and Lilley's trichrome staining.** Histological sections were brought to water as previously described before being placed in Weigert's haematoxylin for 5 minutes and then rinsed in running water. Differentiation, or selective stain removal was performed by incubating the slides in acid alcohol (70% EtOH with 0.5% HCl) for approximately 10. Sections were rinsed in water and subsequently stained in eosin for 5 minutes. This was followed by rapid dehydration by passing through 70%, 90% and 100% alcohol for 2–3 seconds followed by a final 100% alcohol bath for 5 minutes. Incubation in 2 baths of Histo-clear for 10 minutes each was performed dry before mounting with Histomount (Sigma).

**Lilley's trichrome staining.** Histological sections were brought to water as in protocol above, incubated in Weigert's haematoxylin for 5 minutes and rinsed in distilled water. Slides were placed in working strength picric acid solution for 10 minutes, washed in distilled water, and stained in Xylidine Red solution (Sigma) for 1 minute and rinsed in distilled water. Differentiation was performed using a 1% phosphomolybdic acid bath for 10 minutes. Collagen staining was achieved by subsequently staining slides in Aniline Blue solution (Sigma) for 1 minute before being placed in fresh 1% phosphomolybdic acid for 2 minutes and 1% acetic acid for 3 minutes prior to rapid dehydration of samples in 95% and  $2 \times 100\%$  alcohol. Slides were cleared in 2 baths of Histoclear for 10 minutes each before mounting with Histomount.

**Statistical analysis.** Statistical analysis on *in vitro* vector analysis data was performed using an unpaired Student's one-tailed t-test. All data are expressed as mean values  $\pm$  SEM, with each sample being measured at least in triplicate. For *in vivo* data, repeated measurements were analyzed with repeated measures analysis of variance with significance level of p < 0.05. Area under curve data for experiments with two groups was analyzed by Student's one-tailed t-test. For areas under curve derived from two or more groups, one-way analysis of variance with Newman-Keuls post-hoc multiple comparison test was performed.

# References

- 1. Clavien, P. A. et al. Recommendations for liver transplantation for hepatocellular carcinoma: an international consensus conference report. *Lancet Oncol* 13, e11–22, doi: 10.1016/S1470-2045(11)70175-9 (2012).
- 2. Luedde, T. & Schwabe, R. F. NF-kappaB in the liver-linking injury, fibrosis and hepatocellular carcinoma. *Nature reviews. Gastroenterology & hepatology* **8**, 108–118, doi: 10.1038/nrgastro.2010.213 (2011).
- 3. Canbay, A. *et al.* Fas enhances fibrogenesis in the bile duct ligated mouse: a link between apoptosis and fibrosis. *Gastroenterology* **123**, 1323–1330 (2002).
- 4. Gehring, S. et al. Kupffer cells abrogate cholestatic liver injury in mice. Gastroenterology 130, 810-822, doi: 10.1053/j. gastro.2005.11.015 (2006).
- 5. Georgiev, P. et al. Characterization of time-related changes after experimental bile duct ligation. Br J Surg 95, 646–656, doi: 10.1002/bjs.6050 (2008).
- He, F. et al. Myeloid-specific disruption of recombination signal binding protein Jkappa ameliorates hepatic fibrosis by attenuating inflammation through cylindromatosis in mice. Hepatology 61, 303–314, doi: 10.1002/hep.27394 (2015).
- Malato, Y. et al. NF-kappaB essential modifier is required for hepatocyte proliferation and the oval cell reaction after partial hepatectomy in mice. Gastroenterology 143, 1597–1608 e1511, doi: 10.1053/j.gastro.2012.08.030 (2012).
- 8. Kim, K. H., Chen, C. C., Alpini, G. & Lau, L. F. CCN1 induces hepatic ductular reaction through integrin alphavbeta(5)-mediated activation of NF-kappaB. *The Journal of clinical investigation* 125, 1886–1900, doi: 10.1172/JCI79327 (2015).
- 9. Boulter, L. et al. Macrophage-derived Wnt opposes Notch signaling to specify hepatic progenitor cell fate in chronic liver disease. *Nature medicine* 18, 572–579, doi: 10.1038/nm.2667 (2012).
- 10. Buckley, S. M. *et al.* In vivo bioimaging with tissue-specific transcription factor activated luciferase reporters. *Scientific reports* 5, 11842, doi: 10.1038/srep11842 (2015).
- 11. Heinrich, S. et al. Partial bile duct ligation in mice: a novel model of acute cholestasis. Surgery 149, 445–451, doi: 10.1016/j. surg.2010.07.046 (2011).
- 12. Aller, M. A. et al. Microsurgical extrahepatic cholestasis in the rat: a long-term study. Journal of investigative surgery: the official journal of the Academy of Surgical Research 17, 99–104, doi: 10.1080/08941930490422537 (2004).
- 13. Dianat, N. et al. Generation of functional cholangiocyte-like cells from human pluripotent stem cells and HepaRG cells. Hepatology 60, 700–714, doi: 10.1002/hep.27165 (2014).
- Purps, O., Lahme, B., Gressner, A. M., Meindl-Beinker, N. M. & Dooley, S. Loss of TGF-beta dependent growth control during HSC transdifferentiation. *Biochemical and biophysical research communications* 353, 841–847, doi: 10.1016/j.bbrc.2006.12.125
- Osawa, Y. et al. Systemic mediators induce fibrogenic effects in normal liver after partial bile duct ligation. Liver international: official journal of the International Association for the Study of the Liver 26, 1138–1147, doi: 10.1111/j.1478-3231.2006.01346.x
- Kassel, K. M., Sullivan, B. P. & Luyendyk, J. P. Lipopolysaccharide enhances transforming growth factor beta1-induced plateletderived growth factor-B expression in bile duct epithelial cells. *Journal of gastroenterology and hepatology* 27, 714–721, doi: 10.1111/j.1440-1746.2011.06941.x (2012).
- 17. Seyhan, H. et al. Liver fibrogenesis due to cholestasis is associated with increased Smad7 expression and Smad3 signaling. Journal of cellular and molecular medicine 10, 922–932 (2006).
- 18. Dooley, S. et al. Hepatocyte-specific Smad7 expression attenuates TGF-beta-mediated fibrogenesis and protects against liver damage. Gastroenterology 135, 642–659, doi: 10.1053/j.gastro.2008.04.038 (2008).
- 19. Woolbright, B. L. et al. Plasma biomarkers of liver injury and inflammation demonstrate a lack of apoptosis during obstructive cholestasis in mice. *Toxicol Appl Pharmacol* 273, 524–531, doi: 10.1016/j.taap.2013.09.023 (2013).
- 20. Allen, K., Jaeschke, H. & Copple, B. L. Bile acids induce inflammatory genes in hepatocytes: a novel mechanism of inflammation during obstructive cholestasis. *The American journal of pathology* **178**, 175–186, doi: 10.1016/j.ajpath.2010.11.026 (2011).
- 21. Yang, M. *et al.* Osteopontin is an initial mediator of inflammation and liver injury during obstructive cholestasis after bile duct
- ligation in mice. *Toxicol Lett* **224**, 186–195, doi: 10.1016/j.toxlet.2013.10.030 (2014).

  22. Jung, Y. *et al.* Signals from dying hepatocytes trigger growth of liver progenitors. *Gut* **59**, 655–665, doi: 10.1136/gut.2009.204354 (2010)
- Boker, K., Schwarting, G., Kaule, G., Gunzler, V. & Schmidt, E. Fibrosis of the liver in rats induced by bile duct ligation. Effects of inhibition by prolyl 4-hydroxylase. *Journal of hepatology* 13 Suppl 3, S35–40 (1991).
- 24. Patsenker, E. et al. Inhibition of integrin alphavbeta6 on cholangiocytes blocks transforming growth factor-beta activation and retards biliary fibrosis progression. Gastroenterology 135, 660–670, doi: 10.1053/j.gastro.2008.04.009 (2008).
- 25. Wang, B. et al. Role of alphaybeta6 integrin in acute biliary fibrosis. Hepatology 46, 1404-1412, doi: 10.1002/hep.21849 (2007).
- 26. Vanderpool, C. et al. Genetic interactions between hepatocyte nuclear factor-6 and Notch signaling regulate mouse intrahepatic bile duct development in vivo. Hepatology 55, 233–243, doi: 10.1002/hep.24631 (2012).
- 27. Thakurdas, S. M. *et al.* Jagged1 heterozygosity in mice results in a congenital cholangiopathy which is reversed by concomitant deletion of one copy of Poglut1 (Rumi). *Hepatology*, doi: 10.1002/hep.28024 (2015).
- 28. Banerjee, D. et al. Notch suppresses angiogenesis and progression of hepatic metastases. Cancer research 75, 1592–1602, doi: 10.1158/0008-5472.CAN-14-1493 (2015).
- 29. Dill, M. T. et al. Constitutive Notch2 signaling induces hepatic tumors in mice. Hepatology 57, 1607–1619, doi: 10.1002/hep.26165 (2013).
- 30. Chen, Y. et al. Inhibition of Notch signaling by a gamma-secretase inhibitor attenuates hepatic fibrosis in rats. PloS one 7, e46512, doi: 10.1371/journal.pone.0046512 (2012).
- 31. Jors, S. et al. Lineage fate of ductular reactions in liver injury and carcinogenesis. The Journal of clinical investigation 125, 2445–2457, doi: 10.1172/JCI78585 (2015).
- 32. Yang, H. et al. A mouse model of cholestasis-associated cholangiocarcinoma and transcription factors involved in progression. Gastroenterology 141, 378–388, 388 e371–374, doi: 10.1053/j.gastro.2011.03.044 (2011).
- 33. Wang, L. et al. The pleiotropic effects of natural AAV infections on liver-directed gene transfer in macaques. Mol Ther 18, 126–134, doi: 10.1038/mt.2009.245 (2010).

## **Acknowledgements**

JMD, SMB, DP and SNW were funded by the ERC (SOMABIO – 260862), TRM and SNW are funded by the NC3Rs (NC/L001780/1), RK was part-funded by Borne. TRM is also funded by EU Horizon2020 (BATCure – 666918). PA acknowledges South African Medical Research Council and National Research Foundation (NRF, GUNs 81768, 81692, 68339, 85981 & 77954). NCH acknowledges the support of the Wellcome Trust (ref. 103749/Z/14/Z) and CORE/Children's Liver Disease Foundation.

#### **Author Contributions**

T.R.M. and S.N.W. conceived experimental design, J.M.D., S.N.W., S.M.B., D.P. and R.K. contributed data, T.R.M., S.N.W., J.M.D., P.A. and N.C.H. contributed to manuscript development.

# **Additional Information**

Supplementary information accompanies this paper at http://www.nature.com/srep

Competing financial interests: The authors declare no competing financial interests.

How to cite this article: Delhove, J. M. K. M. *et al.* Longitudinal *in vivo* bioimaging of hepatocyte transcription factor activity following cholestatic liver injury in mice. *Sci. Rep.* 7, 41874; doi: 10.1038/srep41874 (2017).

**Publisher's note:** Springer Nature remains neutral with regard to jurisdictional claims in published maps and institutional affiliations.

This work is licensed under a Creative Commons Attribution 4.0 International License. The images or other third party material in this article are included in the article's Creative Commons license, unless indicated otherwise in the credit line; if the material is not included under the Creative Commons license, users will need to obtain permission from the license holder to reproduce the material. To view a copy of this license, visit http://creativecommons.org/licenses/by/4.0/

© The Author(s) 2017